Advances in Nano Research, *Vol. 11, No. 4 (2021) 437-451*
https://doi.org/10.12989/anr.2021.11.4.437

Computer simulation of the nonlinear static behavior of axially functionally graded microtube with porosity

Xiaohuan Li[1§], Tian Wang[1§], Fang Liu[1§] and Zhiwen Zhu[*1, 2]

[1]*School of Mechanical Engineering, Tianjin University, Tianjin 300072, Tianjin, China*
[2]*Tianjin Key Laboratory of Nonlinear Dynamics and Control, Tianjin 300072, Tianjin, China*

(*Received April 22, 2021, Revised August 26, 2021, Accepted August 27, 2021*)

Abstract. Static analysis of microstructures, including bending and buckling, is widely practiced in the fabrication and creation of applications such as actuation, sensing, and energy recovery. This article aims to inquire about the static behavior of non-uniform and imperfect microtubes through a numerical solution. Based on the modified couple stress theory, the first-order shear deformation theory and Von-Karman nonlinear theory, and employing the energy conservation method, the linear and nonlinear governing equations are derived. The porosity-dependent material in both ceramic and metal phases makes the functionally graded materials which are varied along tube length, moreover, cross-sections are also considered uniform and nonuniform via three valuable functions. Finally, the linear and nonlinear equations are solved utilizing the generalized differential quadrature method (GDQM) coupled with the numerical iteration method.

Keywords: axially functionally graded material; buckling; nonlinear effect; non-uniform section; porosity

1. Introduction

A new type of composite material without explicit boundary conditions is a functionally graded material. This type of inhomogeneous structure is the combination of several phases that are minor changes without separation. This proposed combination causes many properties of other materials, including the appropriate flexibility of metal phases thermal and thermal dispersion of ceramic phases, which could be suitably combined in the FGM with metal and ceramic in the unit composition. In short, the aim of creating FGMs is to have the complex properties of several materials in a compound structure. FGMs can increase the thermal resistance of structures by defusing the thermal concentration and thermal stress, so the high-temperature resistance has been seen for these complex functional structures without fumbling structural safety confronted with homogeneous materials. This progress has made FGMs a decent replacement for conventional materials, these enchanting characteristics bring numerous researchists to study this field (Hamidi *et al*. 2015, Allahkarami *et al*. 2017, Ehyaei *et al*. 2017, Akbas 2018a, Arefi and Zenkour 2018, Aydogdu *et al*. 2018, Bensaid *et al*. 2018, Navi *et al*. 2019, Gafour *et al*. 2020, Matouk *et al*. 2020).

Porosity is generally explicitly created to meet practical performance requirements, however, the existence of porosity, voids, or other defects in the production process are inevitable. They have greater design flexibility and are more appropriate than conventional materials, they have played an essential role in various applications, for example, biotechnology and topology optimization chemical techniques. In the imperfect structures, especially in the nonuniform ones, the porosity complicates the mathematical modeling. For example, the porosity existence in the tapered or axially functionally beams and plates, the mentioned structures are switched to two-dimensional graded material, which is more complex than the homogenous ones. So, analyzing the imperfect structures due to the porosity existence in the nonuniform structures has been less attention (Addou Farouk *et al*. 2019, Berghouti *et al*. 2019, Medani *et al*. 2019, Al-Furjan *et al*. 2020, 2021, Bekkaye *et al*. 2020, Kaddari *et al*. 2020, Safarpour *et al*. 2020, Zine *et al*. 2020, Arshid *et al*. 2021, Bellifa *et al*. 2021, Guellil *et al*. 2021, Huang *et al*. 2021a, Tahir *et al*. 2021a, b).

Lately, many researches have shown that the behavior of microstructures to check out the behavior for designing and producing micro-size systems like micro-fluid-flow controllers, energy harvesters, micro-actuator, micro-switches, microsensors, microelectromechanical (MEMS), and atomic force microscopes (AFM) (Huang *et al*. 2019b, Li *et al*. 2019, Wu *et al*. 2020, Zhao *et al*. 2020, Chen *et al*. 2021, Cheng *et al*. 2021, Deng *et al*. 2021, Feng *et al*. 2021, Lv and Liu 2021, Lv *et al*. 2021a, b, Sheng *et al*. 2021, Xie *et al*. 2021, Zhang *et al*. 2021a, b). While the size-effect in the micro-structures have a significant effect, the experimental analysis has also shown the classical theory could not be recommended their results for the small-scale structures, so, in order to implement the length-scale effect on the local and classical theories, a number of higher-order theories have been defined in the past few years. The modified couple stress continuum theory has been the leading theory to explain the impact on a small scale proposed by Yang *et al*. (2002) in order to determine the

*Corresponding author, Ph.D.,
E-mail: zhuzhiwen@tju.edu.cn
§Co-first authors and they had equal contribution.

ISSN: 2287-237X (Print), 2287-2388 (Online)

properties of the small-scale effect in microstructures by impacting the parameters of size effect size and lame constants. According to the laboratory data, the microstructure simulation modified by the couple stress theory is very comparable to the actual structure. It causes many researchers to have determined this higher-order theory to investigate the length-scale effect on small-scale structures (Ghabussi *et al*. 2020, 2021, Lori *et al*. 2020, Shariati *et al*. 2020a, Shokrgozar *et al*. 2020, Chen *et al*. 2021, Jiao *et al*. 2021, Ma *et al*. 2021, Moradi *et al*. 2021, Zhao *et al*. 2021).

Static analysis of macro/, micro/, and nano/-structures is one of the fundamental engineering problems that controls the stability of structures due to internal and external loading, among them, bending and buckling analysis plays an essential role in the control and design of stability and instability of systems. In the past few years, much attention has been paid to the static analysis of small-scale structures. Hou, Wu *et al*. (2021) investigated the linear and nonlinear stability of the nonuniform functionally graded microsize cylindrical beam based on the classical beam theory and using the couple stress theory employing the homotopy perturbation method. Ebrahimi, Hashemabadi *et al*. (2020) analyzed the stability of porosity-dependent functionally graded micro-scale cylindrical shells on the basis of modified couple stress theory and using the analytical procedure. Moayedi *et al*. (2019) studied the dynamic and statical behavior of reinforced microdisk in order to investigate the stability and instability of these structures based on the generalized differential quadrature method. Shariati *et al*. (2020b) described the stability and dynamic of axially functionally graded (AFG) classical beams utilizing the Galerkin method. Bensattalah *et al*. (2018) examined the static analysis of single-walled nanotube in an elastic foundation due to the buckling behavior on the basis of a couple of nonlocal the classic beam theory. Wang *et al*. (2021) studied buckling characteristics of bi-directional functionally graded nano-scale shear deformation tubes applying the nonlocal strain gradient theory and the higher-order tube theory via a numerical approach. Semmah *et al*. (2019) scrutinized the mechanical buckling analysis of nanotubes based on the Timoshenko beam theory and utilizing the nonlocal theory surrounded in a Winkler-type foundation on account of thermal loading. Chemi *et al*. (2015) studied the mechanical buckling load of the chiral nanosize double-walled tube by virtue of the axial compress load found on a couple of nonlocal and first-order shear deformation beam theories. Moreover, Bouhadra *et al*. (2021) utilizing the high-order shear deformation beam theory for the micro and nanoscale structures examined the impact of boundary conditions on the buckling behavior of imperfect FG nanobeam. Nejad and Mohammadimehr (2020) explained the buckling treatment of the porosity-dependent classical sandwich beam via a numerical method surrounded by an elastic foundation. Shafiei and Kazemi (2017) investigated the nonlinear strains of Von-Karman theory on the buckling characteristics of imperfect functionally graded micro-rectangular beams based on the classic beam theory and modified couple stress theory employing the numerical and iteration technique. Also, the thermal buckling behavior of axially functionally graded microbeams considering the nonlinearity impacts was investigated by Shafiei *et al*. (2017a) for fully clamped and fully simply-supported boundary conditions in the thermal conditions and using the temperature-dependents materials. In another research, they Mirjavadi *et al*. (2017b) studied the linear thermal buckling of AFG nanobeams in the thermal environment depend on a couple of nonlocal Eringen theory and classic beam theory applied for various boundary supports. The static behavior of imperfect microsize nonuniform beams, in as much as porous materials, made by bi-directional FG materials by cause of thermal buckling load was examined by Mirjavadi *et al*. (2017a).

Also, many other researchers paid their attention to the buckling behavior of microbeams and microtubes and other applicable structures, nevertheless, the investigation of static analysis of micro-cylindrical beams and tubes via different beams and tubes theory is still needed to develop. Therefore, in this study, the buckling behavior of axially functionally graded microtubes is examined found on the modified couple stress theory and based on the Timoshenko beam theory. The presented structures are considered imperfect as long as the porous materials and the material distributions are varied along the tube length direction. The cross-section is assumed nonuniform hinge on the various and applicable functions of the section. Moreover, the nonlinearity effect of nonlinear Von-Karman theory is coupled to the high-order tube theory that one may examine nonlinear impacts. And finally, the generalized differential quadrature method (GDQM) is connected via an iteration technique to solve the nonlinear governing equations.

2. Mathematical modeling

A uniform cylindrical tube is displayed in Fig. 1, in which the Ri and Ro are the internal and external radius, and L is the tube length. The right tube side is made of pure metal, while the left tube side is made of pure ceramic, so the material distributions changed along the tube length, and the axially graded materials have been made.

In this study, three types of nonuniform radius functions that are made the nonuniform sections, involving the exponential, linear and convex functions, are depicted in Fig. 2, in which the mathematic formulation of them are as follows (Chen *et al*. 2021, Hou *et al*. 2021):

$$R = R_L\left(1 - \varpi\frac{x}{L}\right)^{\xi} \tag{1a}$$

$$R = R_L e^{\left(-\zeta\frac{x}{L}\right)} \tag{1b}$$

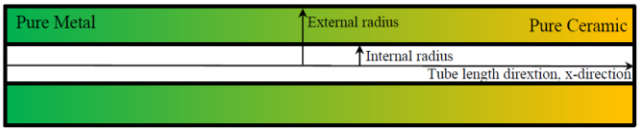

Fig. 1 Schematic of the uniform axially functionally graded tube

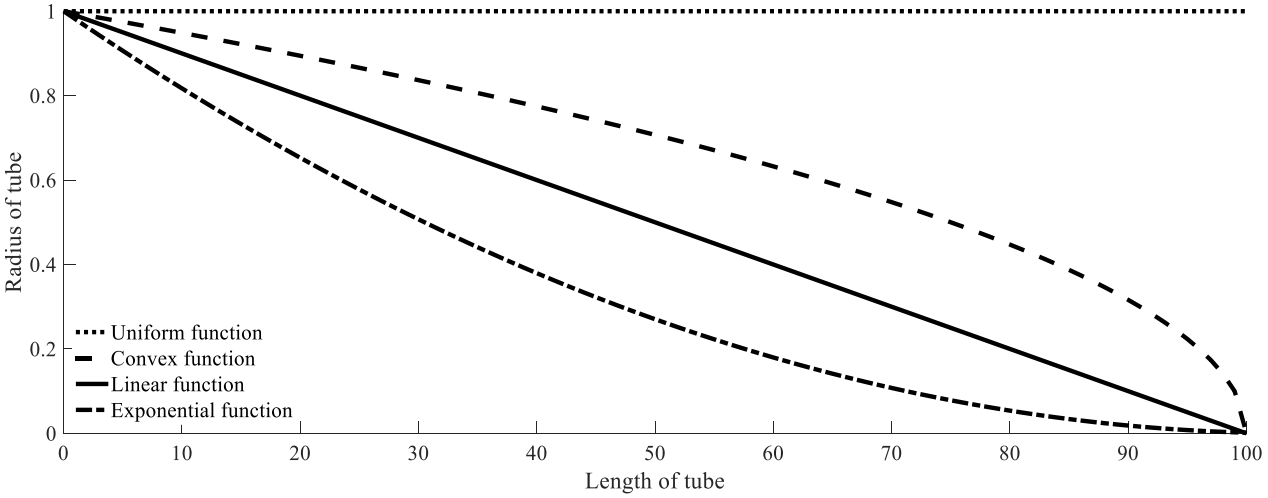

Fig. 2 Different radius functions along the beam length, including the uniform, convex, linear, and exponential types (Hou *et al*. 2021)

where 'R_L' is the tube radius at the left tube side, and 'ϖ' is the 'R_R/R_L', 'ξ' is a parameter to control the radius function that '$\xi = 0$' refers to the uniform section, '$\xi = 1$' is the linear and '$\xi = 0.5$' introduces the convex function. Furthermore, Eq. (1b) describes the mathematical equation of exponential section, which 'ζ' is the nonzero parameter. It should be noted that Eq. (1) supports both inner (Ri) and outer radius (Ro) functions.

The mathematical equations of porosity-dependent axially functionally graded materials properties, including the Poisson ratio (ν) and Young's modulus (E) that are combined with the axially functionally graded materials and the porosity distributions along the radius direction made the two-dimensional functionally graded (2D-FG) materials that are determined as follows (Chen *et al*. 2021, Hou *et al*. 2021):

$$E(x,r) = \left[(E_c - E_m)\left(\frac{x}{L}\right)^p + E_m\right][1 - \rho\Pi(r)] \quad (2a)$$

$$\nu(x,r) = \left[(\nu_c - \nu_m)\left(\frac{x}{L}\right)^p + \nu_m\right][1 - \rho\Pi(r)] \quad (2b)$$

'ρ' is the porous parameter, 'p' is the volume fraction parameter of the FG material, and 'c' refers to the ceramic phase and 'm' regards to the metal phase, which the material properties of ceramic and metal phases are performed in Table 1. Also, function of porosity distribution '$\Pi(r)$' is defined as (Kim *et al*. 2019):

Type1:

$$\Pi(r) = cos\left(\pi\left(\frac{r - Ri}{Ro - Ri}\right)\right) \quad (3a)$$

Type2:

$$E\Pi(r) = cos\left(\frac{\pi}{2}\left(\frac{r - Ri}{Ro - Ri}\right)\right) \quad (3b)$$

Based on the energy conservation method for the statics problem, the governing equations and associated boundary conditions' equations are obtained as follows:

Table 1 Mechanical material properties, involving Young's modulus and Poisson ratio of the ceramic and metal phases (Yang and Shen 2002)

	E (Pa)
SUS304	2.0779e+11
Si_3N_4	3.22269e+11

$$\delta V + \delta S = 0 \quad (4)$$

Here, 'V' is the energy of external work, and 'S' is the strain energy, that the strain energy of small-scale structures on the basis of the modified couple stress theory can be determined as follow (Yang *et al*. 2002):

$$S = \iiint sdv = \frac{1}{2}\iiint (\sigma : \varepsilon + m : \chi)dv \quad (5)$$

where 'ε' is the strain equations of tubes, and according to the first-order shear deformation beam theory of Timoshenko, they are represented as:

$$\varepsilon_{xx} = \frac{\partial u_1}{\partial x} = \frac{\partial u}{\partial x} + \frac{1}{2}\left(\frac{\partial w}{\partial x}\right)^2 + z\frac{\partial \psi}{\partial x} \quad (6a)$$

$$\varepsilon_{xy} = 0 \quad (6b)$$

$$\varepsilon_{xz} = \frac{1}{2}\left(\frac{\partial u_1}{\partial z} + \frac{\partial u_3}{\partial x}\right) = \frac{1}{2}\left(\frac{\partial w}{\partial x} + \psi\right) \quad (6c)$$

where

$$\begin{aligned} u_1(x,y,z) &= u + z\psi(x) \\ u_2(x,y,z) &= 0 \\ u_3(x,y,z) &= w(x) \end{aligned} \quad (7)$$

Here, the displacements element along the x, y, and z-direction are indicated via u1, u2, and u3. 'w' is the lateral deflection and '∂w/∂x' is the rotation angle around the y-direction. Also, 'ψ' is rotation. And stresses are

$$\sigma_{xx} = E\varepsilon_{xx} \quad (8a)$$

$$\sigma_{xy} = G\varepsilon_{xy}, G = \frac{E}{2(1+\nu)} \tag{8b}$$

$$\sigma_{xz} = G\varepsilon_{xy} \tag{8c}$$

On the basis of modified couple stress theory, 'm' is the deviatoric matrices that are defined as follows:

$$m = 2l^2\mu\chi \tag{9}$$

"l" is the length-scale parameter, 'μ' and describe the Lamé constant, and 'χ' is presented as follows:

$$\chi = \frac{1}{2}(\nabla\theta + (\nabla\theta)^T) \tag{10}$$

where

$$\theta = \frac{1}{2}curl(u) \tag{11}$$

Using the Eqs. (9)-(11), the symmetric curvature and the deviatoric tensor are represented as:

$$\chi_{11} = 0, \chi_{22} = 0, \chi_{33} = 0 \tag{12a}$$

$$\chi_{12} = \chi_{21} = \frac{1}{4}\left(\frac{\partial\psi}{\partial x} + \frac{\partial^2 w}{\partial x^2}\right) - \frac{1}{2}\frac{\partial^2 w}{\partial x^2}, \chi_{13} = \chi_{31} = 0 \tag{12b}$$

$$\chi_{23} = \chi_{32} = 0 \tag{12c}$$

The virtual strain energy of first-order micro-scale tube based on the modified couple stress theory is estimated as:

$$\begin{aligned}
\delta S = \iiint \delta s dv = &-\int_0^L \frac{\partial}{\partial x}\left(A_{11}\frac{\partial u}{\partial x}\right) dx\,\delta(u) \\
&+ A_{11}\frac{\partial u}{\partial x}\Big|_0^L \delta(u) + \int_0^L \frac{\partial^2}{\partial x^2}\left(D_{11}\frac{\partial^2 w}{\partial x^2}\right) dx\,\delta(w) \\
&+ D_{11}\frac{\partial^2 w}{\partial x^2}\Big|_0^L \delta\left(\frac{\partial w}{\partial x}\right) - \frac{\partial}{\partial x}\left(D_{11}\frac{\partial^2 w}{\partial x^2}\right)\Big|_0^L \delta(w) \\
&+ \int_0^L \frac{\partial^2}{\partial x^2}\left(D_{11}\frac{\partial^2 w}{\partial x^2}\right) dx\,\delta(w) + D_{11}\frac{\partial^2 w}{\partial x^2}\Big|_0^L \delta\left(\frac{\partial w}{\partial x}\right) \\
&- \frac{\partial}{\partial x}\left(D_{11}\frac{\partial^2 w}{\partial x^2}\right)\Big|_0^L \delta(w) - \int_0^L \frac{\partial}{\partial x}\left(D_{11}\frac{\partial\psi}{\partial x}\right) dx\,\delta(\psi) \\
&- \int_0^L \frac{\partial}{\partial x}\left(D_{11}\frac{\partial^2 w}{\partial x^2}\right) dx\,\delta(\psi) + D_{11}\frac{\partial\psi}{\partial x}\Big|_0^L \delta(\psi) \\
&+ D_{11}\frac{\partial^2 w}{\partial x^2}\Big|_0^L \delta(\psi) + \int_0^L \frac{\partial^2}{\partial x^2}\left(D_{11}\frac{\partial\psi}{\partial x}\right) dx\,\delta(w) \\
&+ D_{11}\frac{\partial\psi}{\partial x}\Big|_0^L \delta\left(\frac{\partial w}{\partial x}\right) - \frac{\partial}{\partial x}\left(D_{11}\frac{\partial\psi}{\partial x}\right)\Big|_0^L \delta(w) \\
&- 2\int_0^L \frac{\partial^2}{\partial x^2}\left(D_{11}\frac{\partial^2 w}{\partial x^2}\right) dx\,\delta(w) - 2\,D_{11}\frac{\partial^2 w}{\partial x^2}\Big|_0^L \delta\left(\frac{\partial w}{\partial x}\right) \\
&+ 2\frac{\partial}{\partial x}\left(D_{11}\frac{\partial^2 w}{\partial x^2}\right)\Big|_0^L \delta(w) + \int_0^L \frac{\partial}{\partial x}\left(D_{11}\frac{\partial^2 w}{\partial x^2}\right) dx\,\delta(\psi) \\
&- D_{11}\frac{\partial^2 w}{\partial x^2}\Big|_0^L \delta(\psi) - \int_0^L \frac{\partial^2}{\partial x^2}\left(D_{11}\frac{\partial\psi}{\partial x}\right) dx\,\delta(w) \\
&- D_{11}\frac{\partial\psi}{\partial x}\Big|_0^L \delta\left(\frac{\partial w}{\partial x}\right) + \frac{\partial}{\partial x}\left(D_{11}\frac{\partial\psi}{\partial x}\right)\Big|_0^L \delta(w) \\
&- \frac{1}{2}\int_0^L \frac{\partial}{\partial x}\left(A_{11}\left(\frac{\partial w}{\partial x}\right)^3\right) dx\,\delta(w) + \frac{A_{11}}{2}\left(\frac{\partial w}{\partial x}\right)^3\Big|_0^L \delta(w) \\
&- \int_0^L \frac{\partial}{\partial x}\left(A_{11}\frac{\partial u}{\partial x}\frac{\partial w}{\partial x}\right) dx\,\delta(w) + A_{11}\frac{\partial u}{\partial x}\frac{\partial w}{\partial x}\Big|_0^L \delta(w) \\
&- \frac{1}{2}\int_0^L \frac{\partial}{\partial x}\left(A_{11}\left(\frac{\partial w}{\partial x}\right)^2\right) dx\,\delta(u) + \frac{A_{11}}{2}\left(\frac{\partial w}{\partial x}\right)^2\Big|_0^L \delta(u) \\
&- \int_0^L \frac{\partial}{\partial x}\left(C_{10}\frac{\partial w}{\partial x}\right) dx\,\delta(w) + C_{10}\frac{\partial w}{\partial x}\Big|_0^L \delta(w) \\
&+ \int_0^L C_{10}\psi\delta(\psi) + C_{10}\frac{\partial w}{\partial x}\delta(\psi)\,dx \\
&- \int_0^L \frac{\partial}{\partial x}(C_{10}(\psi)) dx\,\delta(w) + C_{10}\psi|_0^L\delta(w) \\
&+ l^2\left\{\begin{array}{l}
-\int_0^L \frac{\partial}{\partial x}\left[\frac{1}{4}A_{10}\left(\frac{\partial\psi}{\partial x} + \frac{\partial^2 w}{\partial x^2}\right) - \frac{1}{2}A_{10}\frac{\partial^2 w}{\partial x^2}\right] dx\,\delta(\psi) \\
+\left(\frac{1}{4}A_{10}\left(\frac{\partial\psi}{\partial x} + \frac{\partial^2 w}{\partial x^2}\right) - \frac{1}{2}A_{10}\frac{\partial^2 w}{\partial x^2}\right)\Big|_0^L \delta(\psi) \\
-\frac{\partial}{\partial x}\left[\begin{array}{l}-\frac{1}{4}A_{10}\left(\frac{\partial\psi}{\partial x} + \frac{\partial^2 w}{\partial x^2}\right) \\ +\left(A_{10} - \frac{1}{2}A_{10}\right)\frac{\partial^2 w}{\partial x^2}\end{array}\right]\Big|_0^L \delta(w) \\
+\int_0^L \frac{\partial^2}{\partial x^2}\left[\begin{array}{l}-\frac{1}{4}A_{10}\left(\frac{\partial\psi}{\partial x} + \frac{\partial^2 w}{\partial x^2}\right) \\ +\left(A_{10} - \frac{1}{2}A_{10}\right)\frac{\partial^2 w}{\partial x^2}\end{array}\right] dx\,\delta(w) \\
+\left(A_{10}\left(\frac{\partial\psi}{\partial x} + \frac{\partial^2 w}{\partial x^2}\right) + \left(A_{10} - \frac{1}{2}A_{10}\right)\frac{\partial^2 w}{\partial x^2}\right)\Big|_0^L \delta\left(\frac{\partial w}{\partial x}\right)
\end{array}\right\}
\end{aligned} \tag{13}$$

In which

$$(A_{11}, D_{11}) = \int_A E(x,r)\,(1, z^2) dA \tag{14a}$$

$$(A_{10}, C_{10}) = \int_A G(x,r)\,(1, K_S) dA \tag{14b}$$

Here, 'K_S' is the shear correction factor for the shear deformation theory of circular beams that is calculated as follows (Ma *et al*. 2020):

$$K_S = \frac{6(1+\xi^2)^2(1+\nu)^2}{(7+14\nu+8\nu^2)(1+\xi^2)^2 + 4\xi^2(5+10\nu+4\nu^2)}, \xi = \frac{R_i}{R_O} \tag{15}$$

The virtual energy of external work is defined as follows:

$$\delta V = \iiint \left(\bar{F}\left(\frac{\partial w}{\partial x}\right)\delta\left(\frac{\partial w}{\partial x}\right)\delta w\right) dv \tag{16}$$

$\bar{F}$ is the mechanical buckling load. Finally, by substitution of Eqs. (13) and (16) in Eq. (4), the following Euler-Lagrange equations of first-order shear deformation micro-scale beam theory are obtained as:

$$\frac{\partial}{\partial x}\left(A_{11}\frac{\partial u}{\partial x}\right) + \frac{1}{2}\frac{\partial}{\partial x}\left(A_{11}\left(\frac{\partial w}{\partial x}\right)^2\right) = 0 \tag{17a}$$

$$-\frac{\partial}{\partial x}\left(D_{11}\frac{\partial\psi}{\partial x}\right) - \frac{1}{4}l^2 A_{10}\left(\frac{\partial\psi}{\partial x} - \frac{\partial^2 w}{\partial x^2}\right) + C_{10}\left(\psi + \frac{\partial w}{\partial x}\right) = 0 \tag{17b}$$

$$-\frac{\partial^2}{\partial x^2}\left(\frac{1}{4}l^2A_{10}\left(\frac{\partial\psi}{\partial x}-\frac{\partial^2 w}{\partial x^2}\right)\right)-\frac{\partial}{\partial x}\left(C_{10}\left(\psi+\frac{\partial w}{\partial x}\right)\right)$$
$$-\frac{\partial}{\partial x}\left(\frac{1}{2}A_{11}\left(\frac{\partial w}{\partial x}\right)^2\frac{\partial w}{\partial x}+A_{11}\frac{\partial u}{\partial x}\frac{\partial w}{\partial x}\right)-\bar{F}\frac{\partial^2 w}{\partial x^2}+\bar{q}=0 \quad (17c)$$

The boundary condition for the micro-size Timoshenko tubes are:

$$u=0 \qquad A_{11}\frac{\partial u}{\partial x}+\frac{A_{11}}{2}\left(\frac{\partial w}{\partial x}\right)^2=0 \quad (18a)$$

$$\psi=0 \qquad D_{11}\frac{\partial\psi}{\partial x}+\frac{1}{4}l^2A_{10}\left(\frac{\partial\psi}{\partial x}-\frac{\partial^2 w}{\partial x^2}\right)=0 \quad (18b)$$

$$w=0 \qquad \begin{matrix}+C_{10}\left(\psi+\frac{\partial w}{\partial x}\right)+\frac{1}{4}l^2\frac{\partial}{\partial x}\left(A_{10}\left(\frac{\partial\psi}{\partial x}-\frac{\partial^2 w}{\partial x^2}\right)\right)\\ +A_{11}\left(\frac{1}{2}\left(\frac{\partial w}{\partial x}\right)^2+\frac{\partial u}{\partial x}\right)\frac{\partial w}{\partial x}=0\end{matrix} \quad (18c)$$

3. Numerical solution procedure

The generalized differential quadrature method (GDQM) as the robust method is used in this paper to resolve the linear and nonlinear equations (Ghadiri *et al*. 2016a, b, 2017a, b, Ghadiri and Shafiei 2016a, b, Shafiei *et al*. 2016a, b, c, d, e, f, g, 2017a, 2019, 2020, Ebrahimi *et al*. 2017, Shafiei and Kazemi 2017, Mirjavadi *et al*. 2017a, Azimi *et al*. 2018, Safarpour *et al*. 2020, Chen *et al*. 2021, Hou *et al*. 2021, Huang *et al*. 2021a). Depend on the eigenvalue problem, the general nonlinear equation is solved utilizing the following equation:

$$\{[K]_{Linear}+[K]_{Nonlinear}-\bar{F}[M]\}\{\lambda\}=0 \quad (19)$$

'*K*' is the stiffness matrices, and 'M' is the mass matrices in the static problem, and 'λ' is the mode shapes. Where, the detail of stiffness matrices is defined as follows:

$$[K]_{Linear}=\begin{bmatrix}\frac{\partial}{\partial x}\left(A_{11}\frac{\partial}{\partial x}\right) & 0 & 0\\ 0 & -\frac{\partial}{\partial x}\left(D_{11}\frac{\partial}{\partial x}\right)-\frac{1}{4}l^2A_{10}\frac{\partial}{\partial x}+C_{10} & \frac{1}{4}l^2A_{10}\frac{\partial^2}{\partial x^2}+C_{10}\frac{\partial}{\partial x}\\ 0 & -\frac{\partial^2}{\partial x^2}\left(\frac{1}{4}l^2A_{10}\frac{\partial}{\partial x}\right)-\frac{\partial}{\partial x}(C_{10}) & \frac{\partial^2}{\partial x^2}\left(\frac{1}{4}l^2A_{10}\frac{\partial^2}{\partial x^2}\right)-\frac{\partial}{\partial x}\left(C_{10}\frac{\partial}{\partial x}\right)\end{bmatrix}\begin{Bmatrix}u\\ \psi\\ w\end{Bmatrix} \quad (20a)$$

$$[K]_{Nonlinear}=\begin{bmatrix}0 & 0 & \frac{1}{2}\frac{\partial}{\partial x}\left(A_{11}\frac{\partial w}{\partial x}\frac{\partial}{\partial x}\right)\\ 0 & 0 & 0\\ -\frac{\partial}{\partial x}\left(\frac{1}{2}A_{11}\frac{\partial w}{\partial x}\frac{\partial}{\partial x}\right) & 0 & -\frac{1}{2}\frac{\partial}{\partial x}\left(A_{11}\left(\frac{\partial w}{\partial x}\right)^2\frac{\partial}{\partial x}+A_{11}\frac{\partial u}{\partial x}\frac{\partial}{\partial x}\right)\end{bmatrix}\begin{Bmatrix}u\\ \psi\\ w\end{Bmatrix} \quad (20b)$$

Also, the detail of mass matrices are determined as follows:

$$[M]=\begin{bmatrix}0 & 0 & 0\\ 0 & 0 & 0\\ 0 & 0 & \frac{\partial^2}{\partial x^2}\end{bmatrix}\begin{Bmatrix}u\\ \psi\\ w\end{Bmatrix} \quad (21)$$

According to the GDQ method, the r[th]-order derivative function of P ($\partial^r P/\partial x^r$) is considered as follows:

$$\left.\frac{\partial^r P(x)}{\partial x^r}\right|_{x=x_P}=\sum_{j=1}^{n}C_{ij}^{(r)}P(x_i) \quad (22)$$

here 'n' regards the grid-point number in the tube length direction, and

$$C_{ij}^{(1)}=\frac{\widetilde{M}(x_i)}{(x_i-x_j)\widetilde{M}(x_j)};i,j=1,2,\ldots,n \quad and\ i\neq j$$
$$C_{ij}^{(1)}=-\sum_{j=1,i\neq j}^{n}C_{ij}^{(1)};i=j \quad (23)$$

also $\widetilde{M}(x)$ is:

$$\widetilde{M}(x_i)=\prod_{j=1,j\neq i}^{n}(x_i-x_j) \quad (24)$$

'$C^{(r)}$' is the r[th]-order weighting coefficient that is defined as

$$C_{ij}^{(r)}=r\left[C_{ij}^{(r-1)}C_{ij}^{(1)}-\frac{C_{ij}^{(r-1)}}{(x_i-x_j)}\right];i,j=1,2,\ldots,n,i\neq j \quad and\ 2\leq r\leq n-1$$
$$C_{ii}^{(r)}=-\sum_{j=1,i\neq j}^{n}C_{ij}^{(r)};i,j=1,2,\ldots,n\ and\ 1\leq r\leq n-1 \quad (25)$$

Furthermore, the grid-points are divided as follows:

$$x_i=\frac{L}{2}\left(1-cos\left(\frac{2i-1}{2n}\pi\right)\right)\ i=1,2,3,\ldots,n \quad (26)$$

First, neglecting the nonlinear terms, the linear stiffness matrices based on the GDQM is written as follow:

$$\{[K]_{Linear}-\bar{F}[M]\}\{\lambda\}=0 \quad (27)$$

In the following, the boundary conditions will be assembled with the governing equations. Applying the weight coefficients based on the GDQ technique, the linear buckling load of FG microtube is derived as:

$$\begin{bmatrix}[K_{dd}] & [K_{db}]\\ [K_{bd}] & [K_{bb}]\end{bmatrix}_{Linear}\begin{Bmatrix}\{\lambda_d\}\\ \{\lambda_b\}\end{Bmatrix}=\bar{F}_{linear}\begin{bmatrix}[M_{dd}] & [M_{db}]\\ [M_{bd}] & [M_{bb}]\end{bmatrix}\begin{Bmatrix}\{\lambda_d\}\\ \{\lambda_b\}\end{Bmatrix} \quad (28)$$

where d and b indexes are the domain and boundary, respectively and λ shows the mode shape. Using the linear result of eigenvalue problem (Eq. (28)) and then substitution of linear mode shape, as the initial answer, into the following equation, the initial nonlinear result will be obtained.

$$\begin{bmatrix}[K_{dd}] & [K_{db}]\\ [K_{bd}] & [K_{bb}]\end{bmatrix}_{Linear}\begin{Bmatrix}\{\lambda_d\}\\ \{\lambda_b\}\end{Bmatrix}+\begin{bmatrix}[K_{dd}] & [K_{db}]\\ [K_{bd}] & [K_{bb}]\end{bmatrix}_{Nonlinear}\begin{Bmatrix}\{\lambda_d\}\\ \{\lambda_b\}\end{Bmatrix}=\bar{F}_{nonlinear}\begin{bmatrix}[M_{dd}] & [M_{db}]\\ [M_{bd}] & [M_{bb}]\end{bmatrix}\begin{Bmatrix}\{\lambda_d\}\\ \{\lambda_b\}\end{Bmatrix} \quad (29)$$

Subsequently, the nonlinear calculated results, involving the nonlinear mode shape, will be applied in Eq. (29) to

obtain the new nonlinear results. This cycle will be continued until the results converge. The following relation is used to considering the converge rate.

$$error = \frac{\bar{F}_{i+1} - \bar{F}_i}{\bar{F}_{i+1}}; \qquad i = 1,2,3,\ldots \tag{30}$$

It is repeated until the relative error between the estimated eigenvalue in two consecutive iterations is within the suggested value (0.0001 is a suitable value) (Shafiei *et al*. 2016a, b, c, d, e, f, g).

4. Numerical results and discussion

Before the discussion of the results, the validation of them is necessary. While, in this paper, the buckling behavior of 2D-FG microtubes is investigated for different cross-sections under the clamped and pinned boundary supports; Fig. 3 shows the comparison of presented numerical results of the non-dimensional buckling load of beam and tubes with the results of Reddy (2011). For the most part, some non-dimensional parameters are represented in the following in order to have a better judgment in the comparison and discussion of calculated numerical results.

Nonlinear amplitude of large deflection:

$$W/R = \bar{w}_{nonlinear}\sqrt{\frac{I_0}{A_0 L^2}} \tag{31a}$$

Non-dimensional small-scale effect:

$$\mu = \frac{l}{R_0 o} \tag{31b}$$

Non-dimensional buckling load:

$$F = \bar{F}\frac{L^2}{Ec \times I_0} \tag{31c}$$

where "I_0" is the second moment, and "A_0" is the area of cross-section (at x=0). Also, 'E_C' is Young's modulus of Si_3N_4. The presented comparison in Fig. 3 proves the correctness and validation of computed results, governing equations, and solution procedure. For the cylindrical beam, 'h' is the tube thickness.

Fig. 4 explains the effect of nonlinear deflection (W/R) on the buckling characteristics of fully pinned and clamped tubes versus the different cross-section shapes. It is clearly shown that the increment of nonlinear amplitude enhances the buckling load; in fact, the nonlinear deflection increases the tube stiffness, and the hardening phenomenon is observed due to the nonlinear amplitude. So the stability of tubes improves via nonlinear effects. Furthermore, the uniform section is more stable than the nonuniform one because of its effective thickness. Also, the nonuniform linear section is more stable than the exponential section, and the nonuniform convex section is stable than the nonuniform linear section. The discussed results are valid for both pinned and clamped boundary supports.

The volume fraction (p) impact on the nonlinear buckling load of the axially functionally graded uniform and nonuniform tubes is performed in Fig. 5. Increasing the FG parameter (p) decreases the buckling load because Si3N4 is stiffer than the SUS304, and the volume fraction parameter tends to decrease the tube stiffness. The softening behavior due to the FG parameter is observed, which means FG tubes' stability depreciates by the volume fraction. The mentioned explains confirmed for both clamped and pinned boundaries and also for both uniform and nonuniform sections. As explained, the buckling of the uniform section is higher than the nonuniform, and in the nonuniform types, the nonlinear buckling load of the exponential section is lower than the nonuniform linear section buckling of the convex section is higher than the linear type.

Fig. 6 displays the small-scale effect of modified couple stress effect on the nonlinear buckling load of axially functionally graded microtubes versus the uniform and nonuniform cross-sections for both clamped and pinned boundary conditions. The obtained outputs indicate that the small-scale parameter tends to increases the buckling load, which means the stiffness and stability of the AFG microtube develops by the size-effect parameters. In other words, the hardening characteristics are examined by mu.

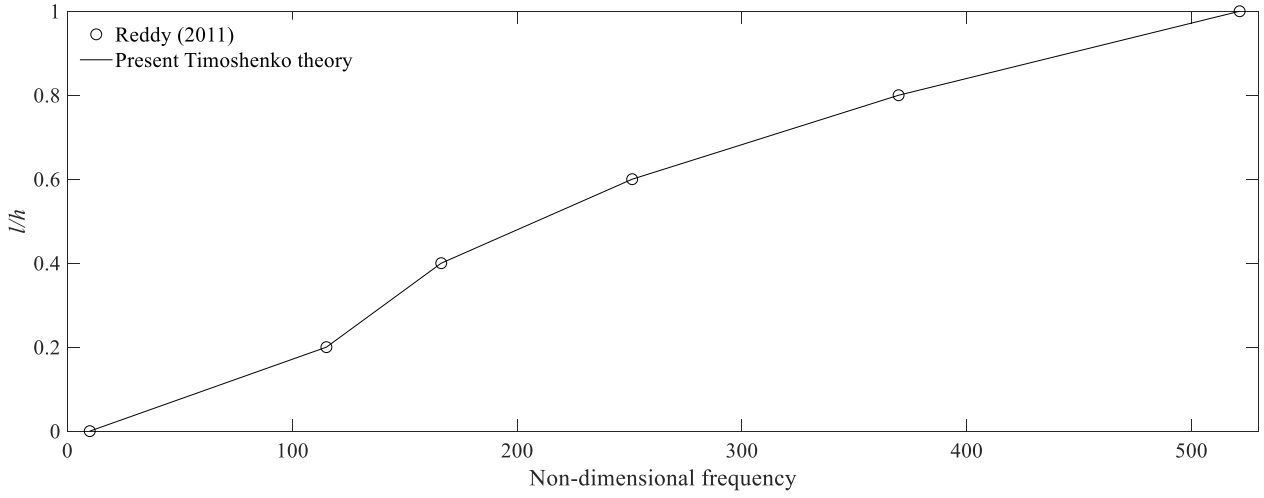

Fig. 3 Comparison of the presented buckling results with the Reddy (2011), to validate the analytical results

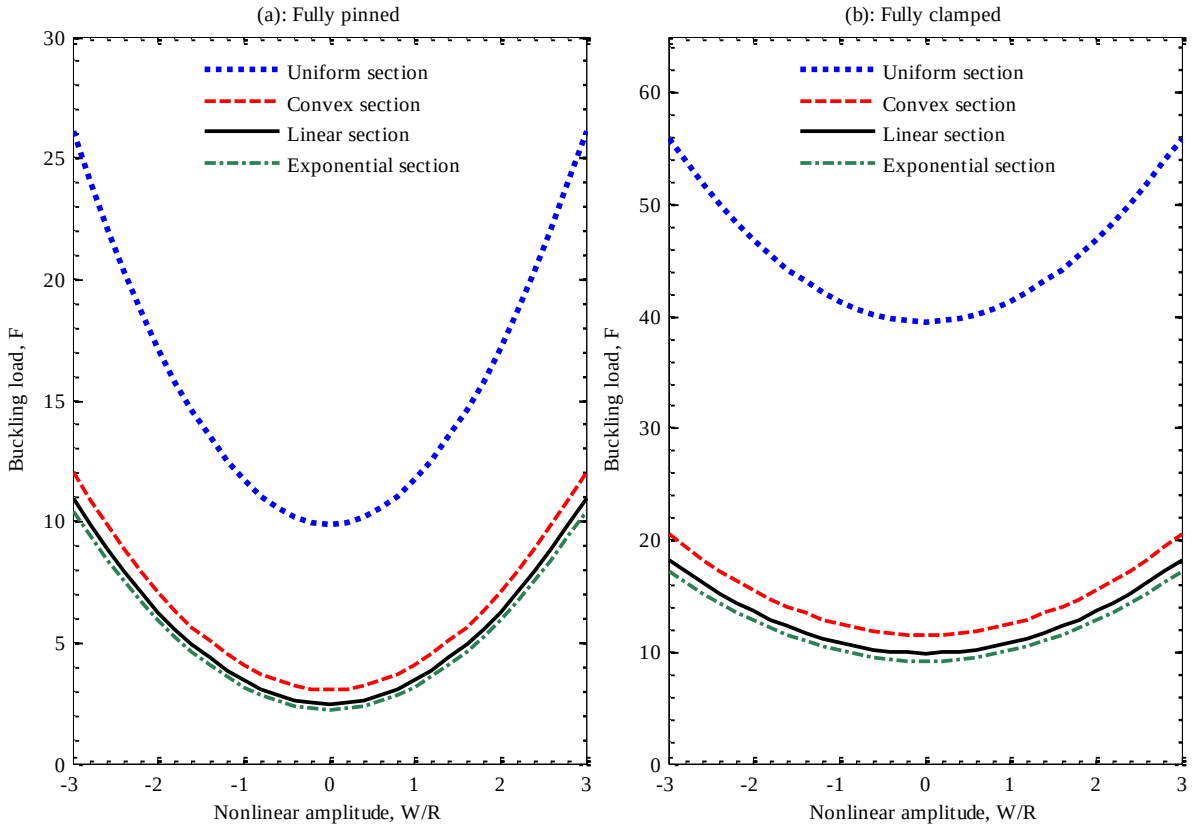

Fig. 4 Nonlinear deflection (W/R) effect on the buckling load of the uniform and nonuniform pinned and clamped tube, L = 40Ro = 80Ri

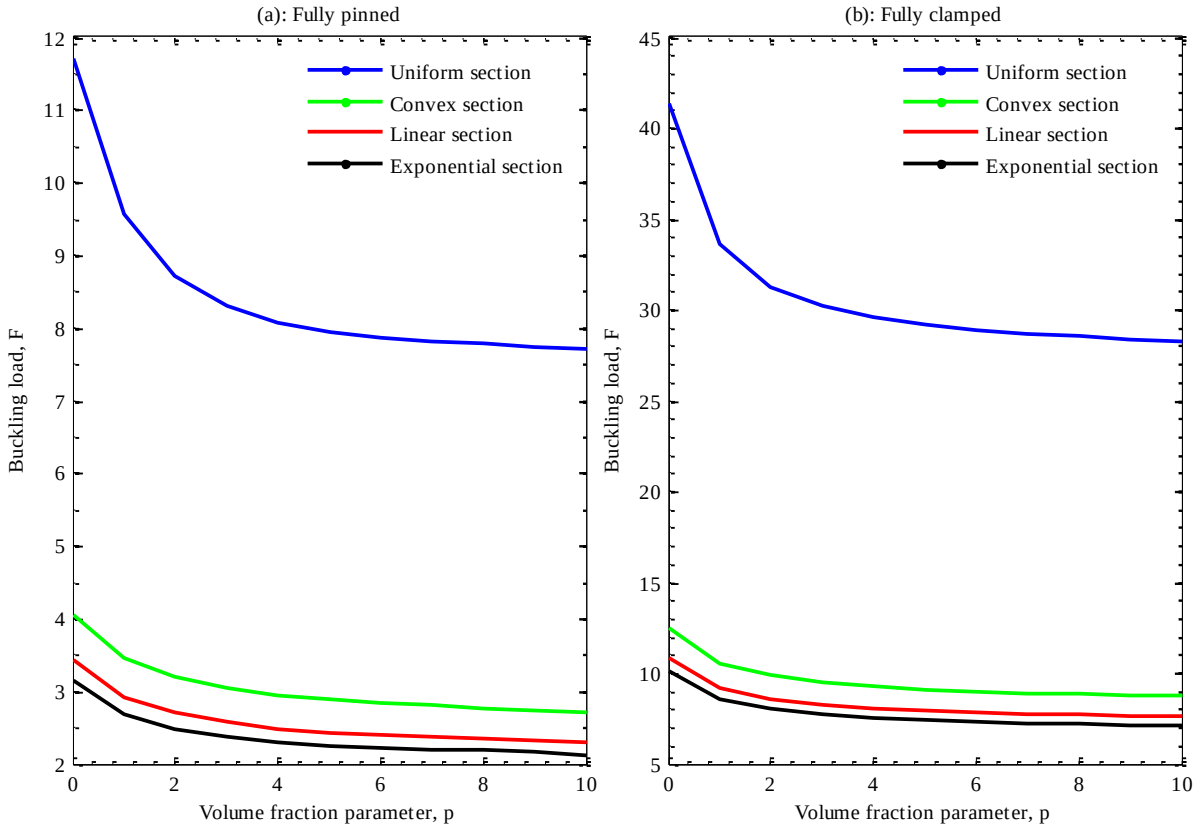

Fig. 5 Volume fraction parameter (p) effect on the buckling load of the uniform and nonuniform pinned and clamped tube, W/R = 1, L = 40Ro = 80Ri

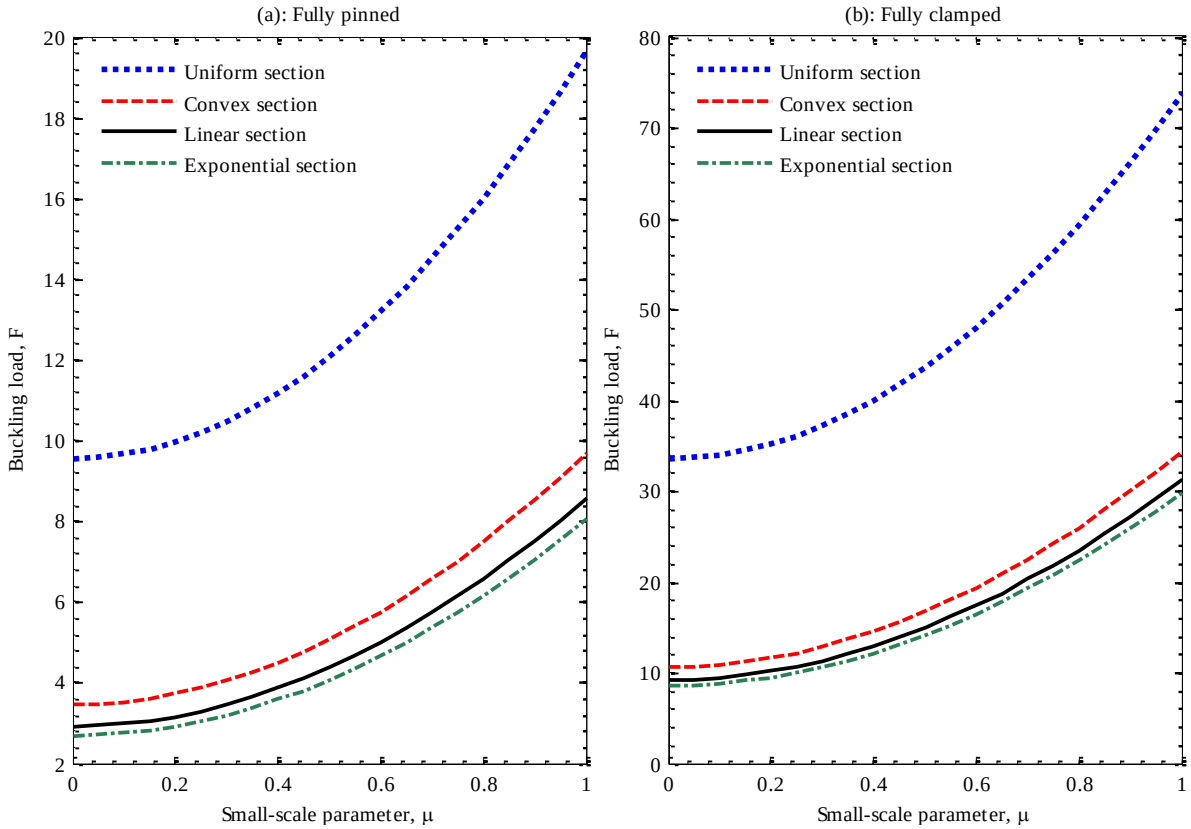

Fig. 6 Length scale (μ) impact on the buckling load of the uniform and nonuniform pinned and clamped tube, W/R = p = 1, L = 40Ro = 80Ri

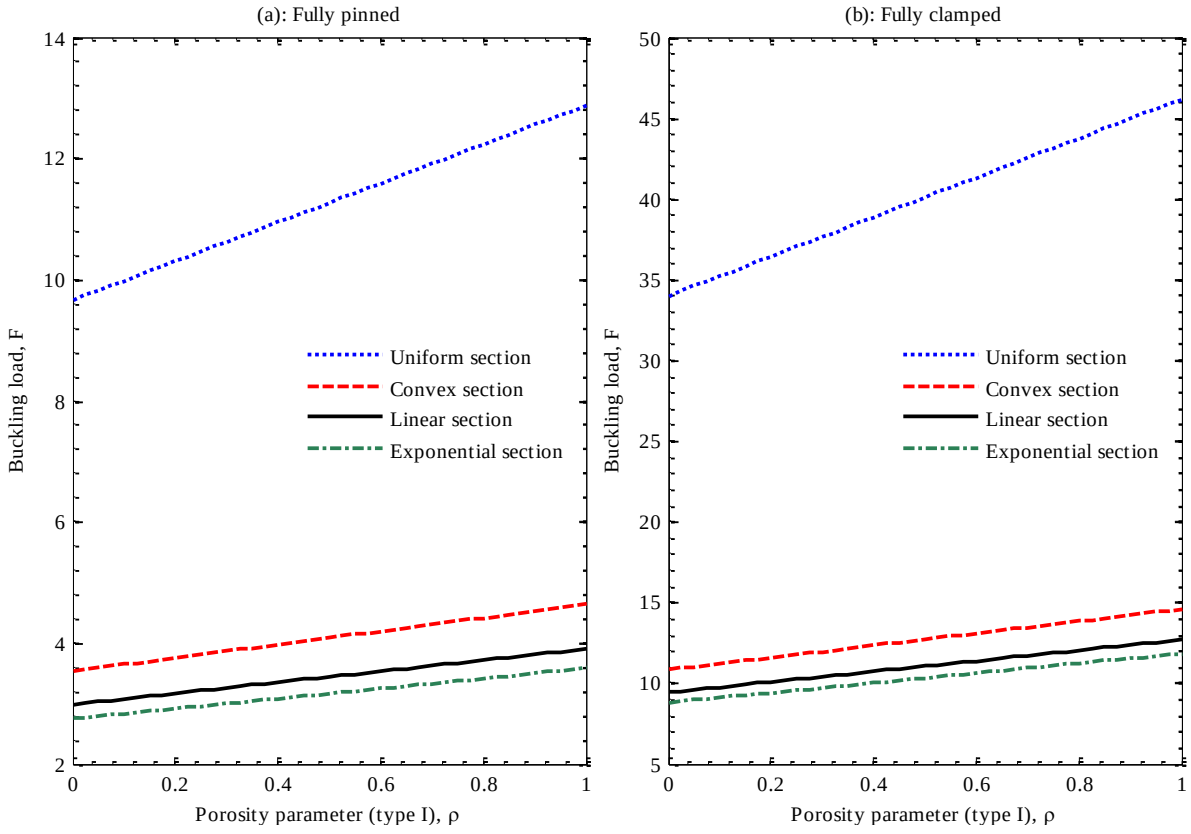

Fig. 7 Porosity impact (type I) on the buckling load of the uniform and nonuniform pinned and clamped tube, W/R = p = 10μ = 1, L = 40Ro = 80Ri

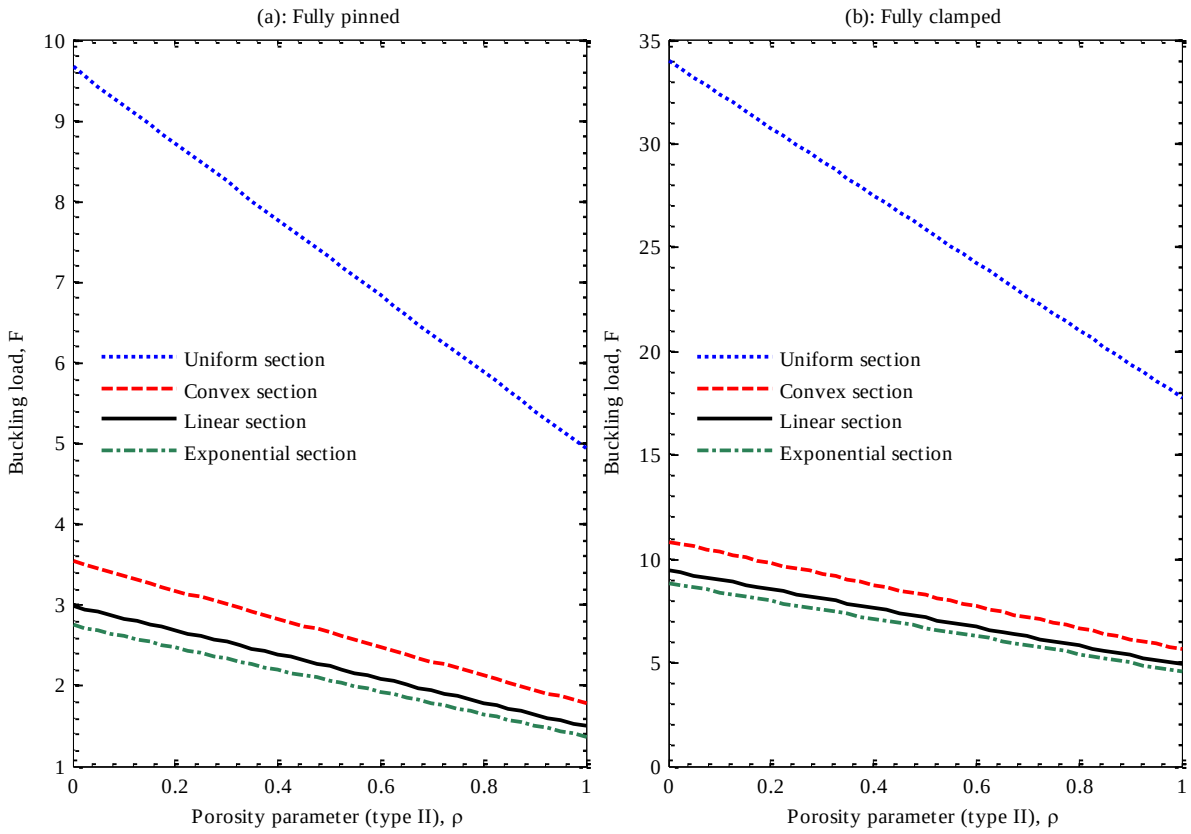

Fig. 8 Porosity impact (type II) on the buckling load of the uniform and nonuniform pinned and clamped tube, W/R = p = 10μ = 1, L = 40Ro = 80Ri

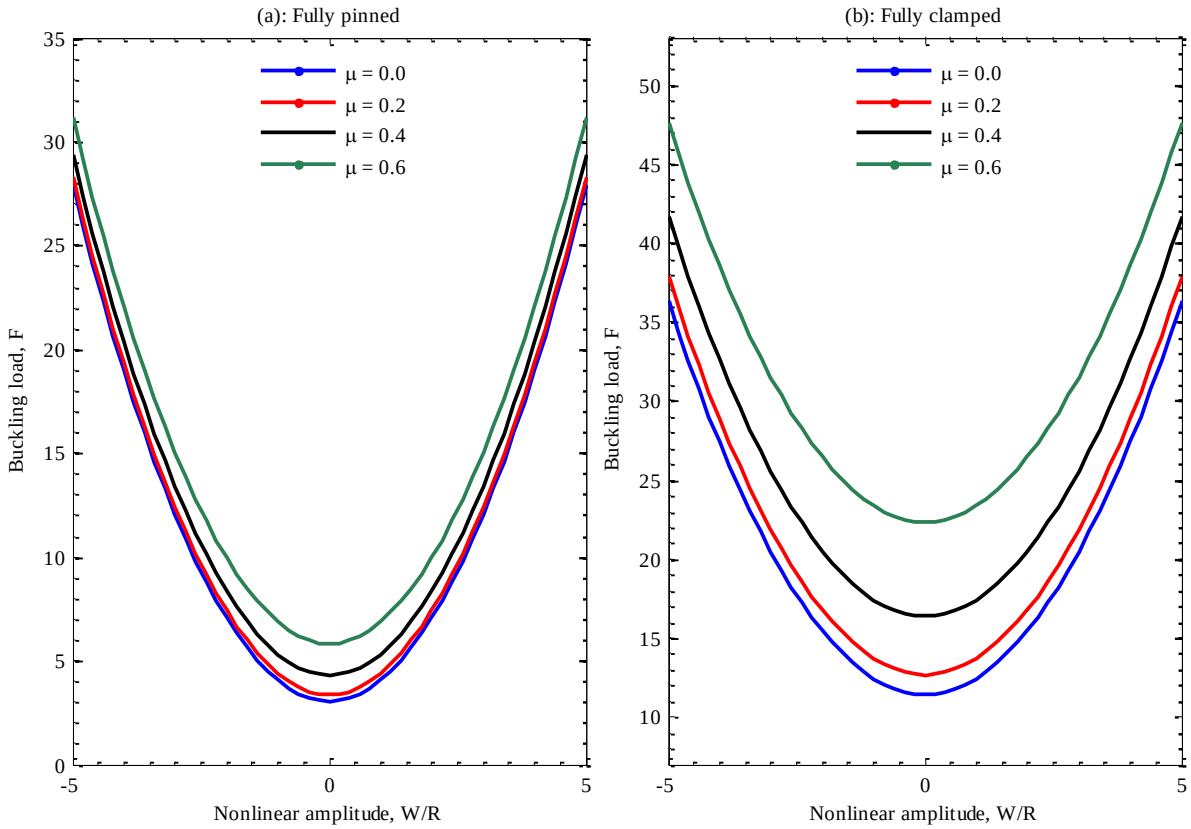

Fig. 9 The small-scale parameter impact on the linear and nonlinear buckling load of fully pinned and fully clamped tube with convex section versus the nonlinear deflection effect, L = 40Ro = 80Ri

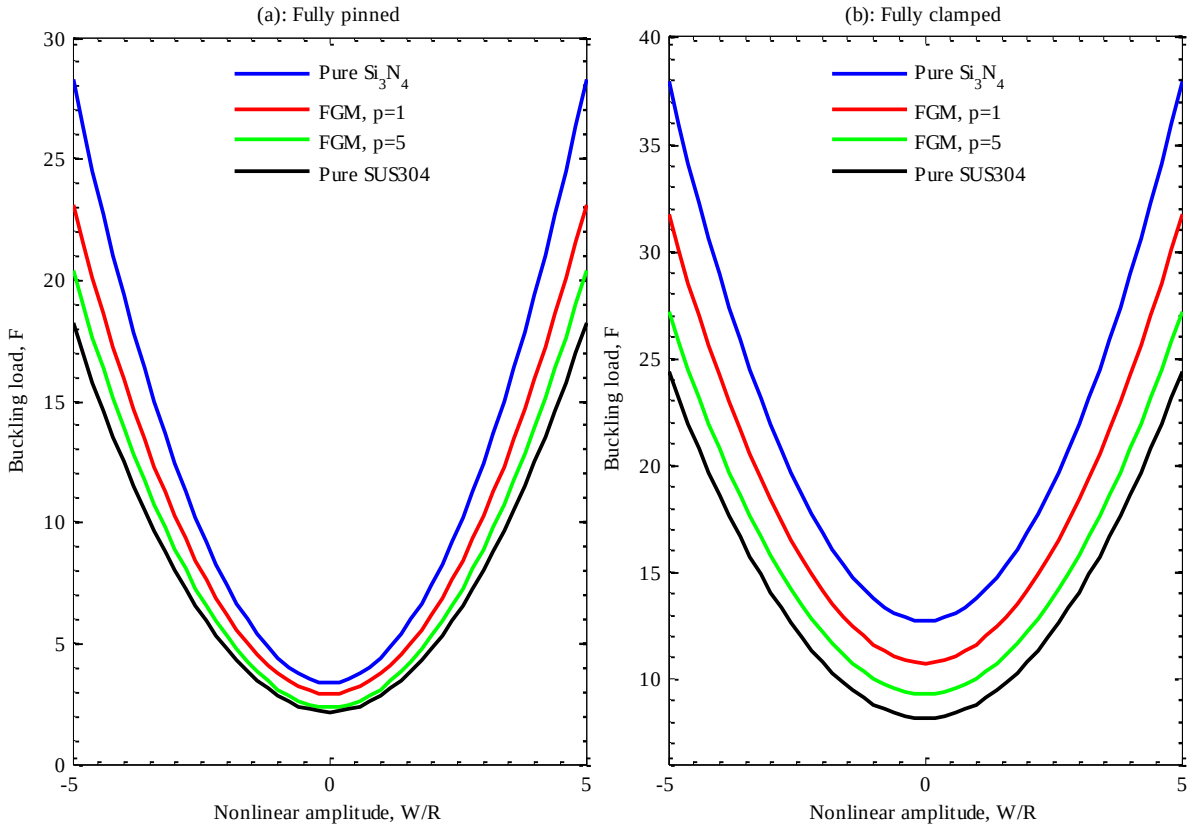

Fig. 10 The volume fraction parameter impact on the linear and nonlinear buckling load of fully pinned and fully clamped microtube with convex section versus the nonlinear deflection effect, μ = 0.2, L = 40Ro = 80Ri

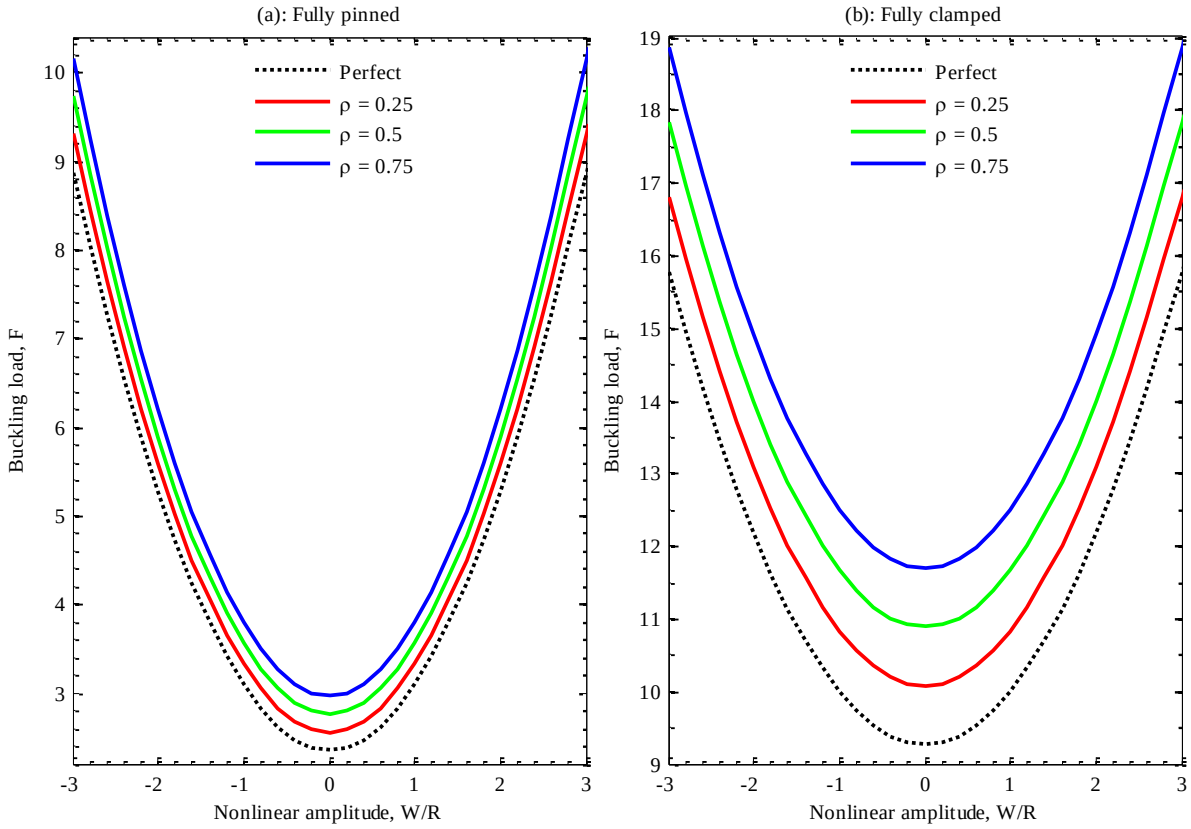

Fig. 11 The porosity impact (distribution of type I) on the linear and nonlinear buckling load of fully pinned and fully clamped 2D-FG microtube with convex section versus the nonlinear deflection effect, p = 5, μ = 0.2, L = 40Ro = 80Ri

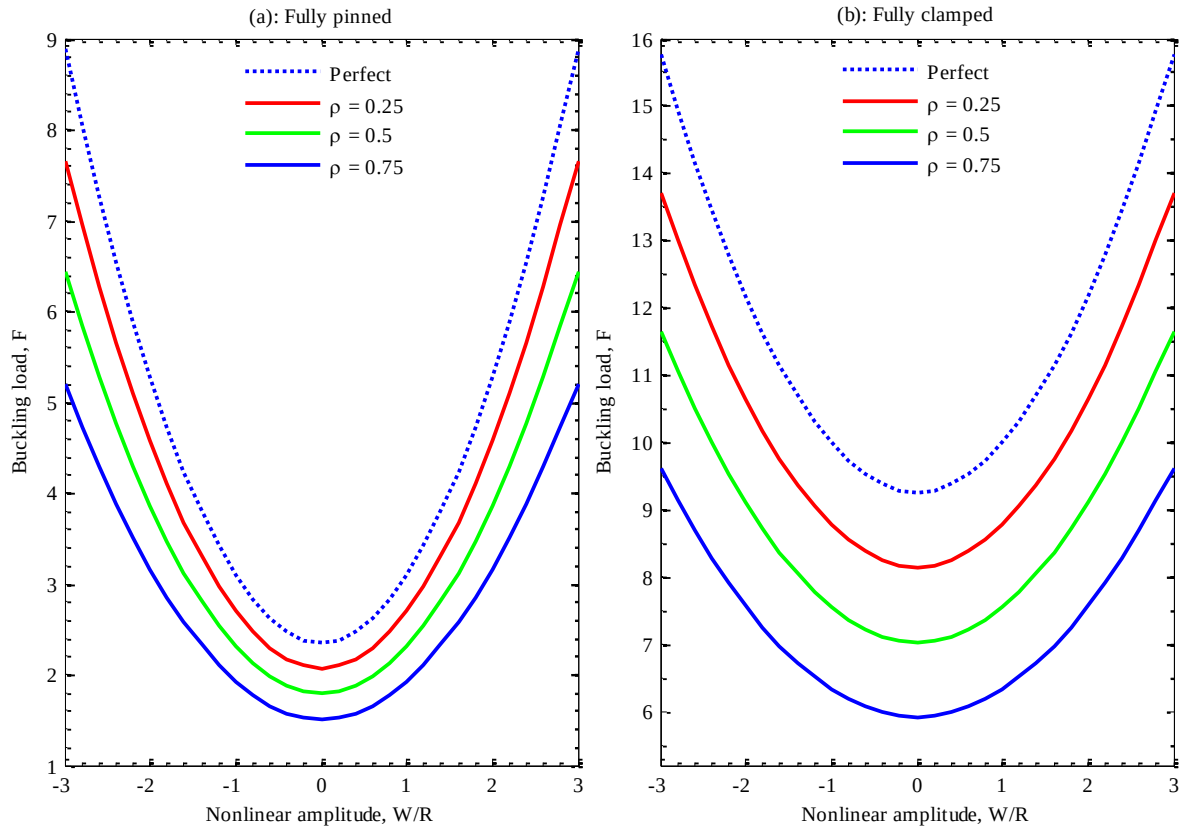

Fig. 12 The porosity impact (distribution of type II) on the linear and nonlinear buckling load of fully pinned and fully clamped 2D-FG microtube with convex section versus the nonlinear deflection effect, p = 5, μ = 0.2, L = 40Ro = 80Ri

The imperfection impact of the porosity parameter (ρ) on the nonlinear buckling load of the 2D-FG fully clamped and fully pinned microtube is manifested in Figs. 7 and 8 versus the uniform and non-uniform cross-section. The imperfection effect is presented in two different porosity distributions, which Figs. 7 and 8 are regarded to type I and type II, respectively. It is recorded that the porosity effect can be lead to both hardening and softening phenomena. In the first type, an increment of the porosity parameter increases the nonlinear buckling load, and stability of the 2D-FG microtube is improved, while in the second type, the stiffness of the 2D-FG microtube limits by the porosity parameter. It is also shown in both porosity distribution types, the impact of the porosity parameter on the nonlinear buckling load is linearly, and the defined describes are recognized in both considered boundary conditions and cross-sections.

The nonlinear impacts, along with the size effect on the nonlinear buckling load of microsize fully pinned and fully clamped tubes, are exposed in Fig. 9. It is shown that the small-scale parameter has more influence on the buckling load in lower nonlinear amplitude values. Moreover, both nonlinear amplitude and small-scale impacts improve the buckling load and stability of microtubes. Also, the fully clamped type is stiffer than the pinned type, and both linear and nonlinear buckling loads of clamped tubes are higher than the pinned ones.

The coupled effect of nonlinear amplitude and volume fraction parameter on the nonlinear buckling load of the microsize clamped and pinned tube is displayed in Fig. 10. The influence of FG parameters on the buckling load enhances via an increment of nonlinear deflection. As explained, an increment of the FG parameter decreases the linear and nonlinear buckling load that leads to limiting the microtubes' stability.

Figs. 11 and 12 explain the nonlinear amplitude and the porosity impact on the linear and nonlinear buckling characteristics of the 2D-FG microtube for pinned and clamped boundary conditions. Fig. 11 presents the buckling behavior of the imperfect tube versus the porosity distributions of type I, that increment of porosity parameter improves the stability of the 2D-FG microtube. In contrast, the second type of porosity distribution was rendered in Fig. 12 that the softening behavior is seen due to the porosity impact. Furthermore, the nonlinear deflection plays an important role in the porosity impact on the linear and nonlinear buckling load. In type I of porosity distributions, the nonlinear amplitude limits the porosity effect on the buckling load, while, in the second porosity distribution type, the nonlinear deflection amplifies the porosity impact on the linear and nonlinear buckling load.

5. Conclusions

The contemporary study framework is the nonlinear

buckling characteristics of the cylindrical micro-scale functionally graded tube under the external compress load based on the modified couple stress theory in conjunction with the first-order shear deformation beam theory along with the Von-Kármán theory. The nonlinear governing equations and boundary conditions equations have been derived by applying the energy conservation methods, which were solved by employing the generalized differential quadrature method. The obtained results were presented for both pinned and clamped boundary support types; that the main findings are:

• The uniform section is more stable than the non-uniform section, and the linear and nonlinear buckling load of uniform tubes contains a higher value than the non-uniform type.

• In the non-uniform sections, the convex type is more stable than the linear section, and the exponential section is unstable than the linear type.

• The nonlinear deflection raises the buckling load that leads to improving the tube stiffness.

• The volume fraction decreases the linear and nonlinear buckling load because the Si_3N_4 is stiffer than SUS304.

• The modified couple stress parameter leads to the hardening phenomena, and an increment of size effect parameter predicts the higher linear and nonlinear buckling load.

• The porosity can be lead to both softening and hardening characteristics based on the porosity distribution type. Because of stiffening behavior, Type-I of porosity distribution tends to enhance the linear and nonlinear buckling load, and in contrast, type-II leads to limiting the buckling load.

Acknowledgement

This work was supported by Natural Science Foundation of China (NSFC) through Grant Nos.11872266, 51875396 and 12021002

References

Addou F.Y., Meradjah, M., Bousahla Abdelmoumen, A., Benachour, A., Bourada, F., Tounsi, A. and Mahmoud, S.R. (2019), "Influences of porosity on dynamic response of FG plates resting on Winkler/Pasternak/Kerr foundation using quasi 3D HSDT", *Comput. Concrete*, **24**(4), 347-367. http://doi.org/10.12989/CAC.2019.24.4.347.

Akbas, S.D. (2018a), "Forced vibration analysis of cracked functionally graded microbeams", *Adv. Nano Res.*, **6**(1), 39-55. http://doi.org/10.12989/anr.2018.6.1.039.

Akbaş, Ş.D. (2018b), "Bending of a cracked functionally graded nanobeam", *Adv. Nano Res.*, **6**(3), 219-243. http://doi.org/10.12989/anr.2018.6.3.219.

Al-Furjan, M.S.H., Habibi, M., Ni, J., Jung, D.w. and Tounsi, A. (2020), "Frequency simulation of viscoelastic multi-phase reinforced fully symmetric systems", *Eng. Comput.*, 1-17. http://doi.org/10.1007/s00366-020-01200-x).

Al-Furjan, M.S.H., Hatami, A., Habibi, M., Shan, L. and Tounsi, A. (2021), "On the vibrations of the imperfect sandwich higher-order disk with a lactic core using generalize differential quadrature method", *Compos, Struct.*, **257**, 113150. https://doi.org/10.1016/j.compstruct.2020.113150.

Allahkarami, F., Nikkhah-Bahrami, M. and Saryazdi, M.G. (2017), "Damping and vibration analysis of viscoelastic curved microbeam reinforced with FG-CNTs resting on viscoelastic medium using strain gradient theory and DQM", *Steel Compos. Struct.*, **25**(2), 141-155. https://doi.org/10.12989/scs.2017.25.2.141.

Arefi, M. and Zenkour, A.M. (2018), "Free vibration analysis of a three-layered microbeam based on strain gradient theory and three-unknown shear and normal deformation theory", *Steel Compos. Struct.*, **26**(4), 421-437. https://doi.org/10.12989/scs.2018.26.4.421.

Arshid, E., Khorasani, M., Soleimani-Javid, Z., Amir, S. and Tounsi, A. (2021), "Porosity-dependent vibration analysis of FG microplates embedded by polymeric nanocomposite patches considering hygrothermal effect via an innovative plate theory", *Eng. Comput.*, 1-22. http://doi.org/10.1007/s00366-021-01382-y.

Aydogdu, M., Arda, M. and Filiz, S. (2018), "Vibration of axially functionally graded nano rods and beams with a variable nonlocal parameter", *Adv. Nano Res.*. **6**(3), 257-278. http://doi.org/10.12989/anr.2018.6.3.257.

Azimi, M., Mirjavadi, S.S., Shafiei, N., Hamouda, A.M.S. and Davari, E. (2018), "Vibration of rotating functionally graded Timoshenko nano-beams with nonlinear thermal distribution", *Mech. Adv. Mater. Struct.*, **25**(6), 467-480. http://doi.org/10.1080/15376494.2017.1285455).

Bekkaye, T.H.L., Fahsi, B., Bousahla, A.A., Bourada, F., Tounsi, A., Benrahou, K.H., Tounsi, A. and Al-Zahrani, M.M. (2020), "Porosity-dependent mechanical behaviors of FG plate using refined trigonometric shear deformation theory", *Comput. Concrete*. **26**(5), 439-450. http://doi.org/10.12989/CAC.2020.26.5.439.

Bellifa, H., Selim, M.M., Chikh, A., Bousahla, A.A., Bourada, F., Tounsi, A., Benrahou, K.H., Al-Zahrani, M.M. and Tounsi, A. (2021), "Influence of porosity on thermal buckling behavior of functionally graded beams", *Smart Struct. Syst.*, **27**(4), 719-728. https://doi.org/10.12989/sss.2021.27.4.719.

Bensaid, I., Bekhadda, A. and Kerboua, B. (2018), "Dynamic analysis of higher order shear-deformable nanobeams resting on elastic foundation based on nonlocal strain gradient theory", *Adv. Nano Res.*. **6**(3), 279. http://doi.org/10.12989/anr.2018.6.3.279.

Bensattalah, T., Bouakkaz, K., Zidour, M. and Daouadji, T.H. (2018), "Critical buckling loads of carbon nanotube embedded in Kerr's medium", *Adv. Nano Res.*, **6**(4), 339-356. http://doi.org/10.12989/anr.2018.6.4.339.

Berghouti, H., Adda Bedia, E.A., Benkhedda, A. and Tounsi, A. (2019), "Vibration analysis of nonlocal porous nanobeams made of functionally graded material", *Adv. Nano Res.*, **7**(5), 351-364. http://doi.org/10.12989/ANR.2019.7.5.351.

Bouhadra, A., Menasria, A. and Rachedi, M.A. (2021), "Boundary conditions effect for buckling analysis of porous functionally graded nanobeam", *Adv. Nano Res.*, **10**(4), 313-325. https://doi.org/10.12989/anr.2021.10.4.313.

Chemi, A., Heireche, H., Zidour, M., Rakrak, K. and Bousahla, A.A. (2015), "Critical buckling load of chiral double-walled carbon nanotube using non-local theory elasticity", *Adv. Nano Res.*, **3**(4), 193-206. http://doi.org/10.12989/anr.2015.3.4.193).

Chen, R., Cheng, Y., Wang, P., Wang, Y., Wang, Q., Yang, Z., Tang, C., Xiang, S., Luo, S., Huang, S. and Su, C. (2021), "Facile synthesis of a sandwiched Ti_3C_2Tx MXene/nZVI/ fungal hypha nanofiber hybrid membrane for enhanced removal of Be(II) from $Be(NH_2)_2$ complexing solutions", *Chem. Eng. J.*, **421**, 129682. https://doi.org/10.1016/j.cej.2021.129682.

Cheng, H., Li, T., Li, X., Feng, J., Tang, T. and Qin, D. (2021), "Facile synthesis of Co_9S_8 nanocages as an electrochemical

sensor for luteolin detection", *J. Electrochem. Soc.*, **168**(8), 087504. http://doi.org/10.1149/1945-7111/ac1813.

Deng, H., Chen, Y., Jia, Y., Pang, Y., Zhang, T., Wang, S. and Yin, L. (2021), "Microstructure and mechanical properties of dissimilar NiTi/Ti6Al4V joints via back-heating assisted friction stir welding", *J. Manuf. Proc.*, **64**, 379-391. https://doi.org/10.1016/j.jmapro.2021.01.024.

Ebrahimi, F., Shafiei, N., Kazemi, M. and Mousavi Abdollahi, S.M. (2017), "Thermo-mechanical vibration analysis of rotating nonlocal nanoplates applying generalized differential quadrature method", *Mech. Adv. Mater. Struct.*, **24**(15), 1257-1273. http://doi.org/10.1080/15376494.2016.1227499.

Ebrahimi, F., Hashemabadi, D., Habibi, M. and Safarpour, H. (2020), "Thermal buckling and forced vibration characteristics of a porous GNP reinforced nanocomposite cylindrical shell", *Microsyst. Technol.*, **26**(2), 461-473. http://doi.org/10.1007/s00542-019-04542-9.

Ehyaei, J., Akbarshahi, A. and Shafiei, N. (2017), "Influence of porosity and axial preload on vibration behavior of rotating FG nanobeam", *Adv. Nano Res.*, **5**(2), 141-169. http://doi.org/10.12989/anr.2017.5.2.141.

Feng, S., Zuo, C., Zhang, L., Yin, W. and Chen, Q. (2021), "Generalized framework for non-sinusoidal fringe analysis using deep learning", *Photon. Res.*, **9**(6), 1084-1098. http://doi.org/10.1364/PRJ.420944.

Gafour, Y., Hamidi, A., Benahmed, A., Zidour, M. and Bensattalah, T. (2020), "Porosity-dependent free vibration analysis of FG nanobeam using non-local shear deformation and energy principle", *Adv. Nano Res.*, **8**(1), 37-47. https://doi.org/10.12989/anr.2020.8.1.037.

Ghabussi, A., Habibi, M., NoormohammadiArani, O., Shavalipour, A., Moayedi, H. and Safarpour, H. (2020), "Frequency characteristics of a viscoelastic graphene nanoplatelet–reinforced composite circular microplate", *J. Vib. Control.*, **27**(1-2), 101-118. http://doi.org/10.1177/1077546320923930.

Ghabussi, A., Ashrafi, N., Shavalipour, A., Hosseinpour, A., Habibi, M., Moayedi, H., Babaei, B. and Safarpour, H. (2021), "Free vibration analysis of an electro-elastic GPLRC cylindrical shell surrounded by viscoelastic foundation using modified length-couple stress parameter", *Mech. Based Des. Struct.*, **49**(5), 738-762. http://doi.org/10.1080/15397734.2019.1705166.

Ghadiri, M. and Shafiei, N. (2016a), "Nonlinear bending vibration of a rotating nanobeam based on nonlocal Eringen's theory using differential quadrature method", *Microsyst. Technol.*, **22**(12), 2853-2867. http://doi.org/10.1007/s00542-015-2662-9.

Ghadiri, M. and Shafiei, N. (2016b), "Vibration analysis of a nano-turbine blade based on Eringen nonlocal elasticity applying the differential quadrature method", *J. Vib. Control.*, **23**(19), 3247-3265. http://doi.org/10.1177/1077546315627723.

Ghadiri, M., Hosseini, S.H.S. and Shafiei, N. (2016a), "A power series for vibration of a rotating nanobeam with considering thermal effect", *Mech. Adv. Mater. Struct.*, **23**(12), 1414-1420. http://doi.org/10.1080/15376494.2015.1091527.

Ghadiri, M., Shafiei, N. and Alireza Mousavi, S. (2016b), "Vibration analysis of a rotating functionally graded tapered microbeam based on the modified couple stress theory by DQEM", *Appl. Phys. A.*, **122**(9), 837. http://doi.org/10.1007/s00339-016-0364-5.

Ghadiri, M., Shafiei, N. and Alavi, H. (2017a), "Thermo-mechanical vibration of orthotropic cantilever and propped cantilever nanoplate using generalized differential quadrature method", *Mech. Adv. Mater. Struct.*, **24**(8), 636-646. http://doi.org/10.1080/15376494.2016.1196770.

Ghadiri, M., Shafiei, N. and Babaei, R. (2017b), "Vibration of a rotary FG plate with consideration of thermal and Coriolis effects", *Steel Compos. Struct.*, **25**(2), 197-207. http://doi.org/10.12989/SCS.2017.25.2.197.

Guellil, M., Saidi, H., Bourada, F., Bousahla, A.A., Tounsi, A., Al-Zahrani, M.M., Hussain, M. and Mahmoud, S. (2021), "Influences of porosity distributions and boundary conditions on mechanical bending response of functionally graded plates resting on Pasternak foundation", *Steel Compos. Struct.*, **38**(1), 1-15. https://doi.org/10.12989/scs.2021.38.1.001.

Hamidi, A., Houari, M.S.A., Mahmoud, S. and Tounsi, A. (2015), "A sinusoidal plate theory with 5-unknowns and stretching effect for thermomechanical bending of functionally graded sandwich plates", *Steel Compos. Struct.*, **18**(1), 235-253. https://doi.org/10.12989/scs.2015.18.1.235.

Hou, F., Wu, S., Moradi, Z. and Shafiei, N. (2021), "The computational modeling for the static analysis of axially functionally graded micro-cylindrical imperfect beam applying the computer simulation", *Eng. Comput.*, 1-19. http://doi.org/10.1007/s00366-021-01456-x.

Huang, X., Zhang, Y., Moradi, Z. and Shafiei, N. (2021a), "Computer simulation via a couple of homotopy perturbation methods and the generalized differential quadrature method for nonlinear vibration of functionally graded non-uniform micro-tube", *Eng. Comput.*, 1-18. http://doi.org/10.1007/s00366-021-01395-7.

Huang, Z.Q., Yi, S.H., Chen, H.X. and He, X.Q. (2019b), "Parameter analysis of damaged region for laminates with matrix defects", *J. Sandw. Struct. Mater.*, **23**(2), 580-620. http://doi.org/10.1177/1099636219842290.

Jiao, J., Ghoreishi, S.M., Moradi, Z. and Oslub, K. (2021), "Coupled particle swarm optimization method with genetic algorithm for the static–dynamic performance of the magneto-electro-elastic nanosystem", *Eng. Comput.*, 1-15. http://doi.org/10.1007/s00366-021-01391-x.

Kaddari, M., Kaci, A., Bousahla Abdelmoumen, A., Tounsi, A., Bourada, F., Tounsi, A., Bedia, E.A.A. and Al-Osta, M.A. (2020), "A study on the structural behaviour of functionally graded porous plates on elastic foundation using a new quasi-3D model: Bending and free vibration analysis", *Comput. Concrete*, **25**(1), 37-57. http://doi.org/10.12989/CAC.2020.25.1.037.

Kim, J., Żur, K.K. and Reddy, J.N. (2019), "Bending, free vibration, and buckling of modified couples stress-based functionally graded porous micro-plates", *Compos. Struct.*, **209**, 879-888. https://doi.org/10.1016/j.compstruct.2018.11.023.

Li, X., Shi, T., Li, B., Chen, X., Zhang, C., Guo, Z. and Zhang, Q. (2019), "Subtractive manufacturing of stable hierarchical micro-nano structures on AA5052 sheet with enhanced water repellence and durable corrosion resistance", *Mater. Design*, **183**, 108152. https://doi.org/10.1016/j.matdes.2019.108152.

Lori, E.S., Ebrahimi, F., Supeni, E.E.B., Habibi, M. and Safarpour, H. (2020), "Frequency characteristics of a GPL-reinforced composite microdisk coupled with a piezoelectric layer", *Eur. Phys. J. Plus.*, **135**(2), 144. http://doi.org/10.1140/epjp/s13360-020-00217-x.

Lv, S. and Liu, Y. (2021), "PLVA: Privacy-preserving and lightweight V2I authentication protocol", *IEEE T. Intell. Transp.*, 1-7. http://doi.org/10.1109/TITS.2021.3059638.

Lv, Z., Chen, D. and Wang, Q. (2021a), "Diversified technologies in internet of vehicles under intelligent edge computing", *IEEE T. Intell. Transp.*, **22**(4), 2048-2059. http://doi.org/10.1109/TITS.2020.3019756.

Lv, Z., Lou, R. and Singh, A.K. (2021b), "AI empowered communication systems for intelligent transportation systems", *IEEE T. Intell. Transp.*, **22**(7), 4579-4587. http://doi.org/10.1109/TITS.2020.3017183.

Ma, W.L., Li, X.F. and Lee, K.Y. (2020), "Third-order shear deformation beam model for flexural waves and free vibration of pipes", *J. Acoust. Soc. Am.*, **147**(3), 1634-1647. http://doi.org/10.1121/10.0000855.

Ma, L., Liu, X. and Moradi, Z. (2021), "On the chaotic behavior of graphene-reinforced annular systems under harmonic excitation", *Eng. Comput.*, 1-25. http://doi.org/10.1007/s00366-020-01210-9.

Matouk, H., Bousahla, A.A., Heireche, H., Bourada, F., Bedia, E., Tounsi, A., Mahmoud, S., Tounsi, A. and Benrahou, K. (2020), "Investigation on hygro-thermal vibration of P-FG and symmetric S-FG nanobeam using integral Timoshenko beam theory", *Adv. Nano Res.*, **8**(4), 293-305. https://doi.org/10.12989/anr.2020.8.4.293.

Medani, M., Benahmed, A., Zidour, M., Heireche, H., Tounsi, A., Bousahla, A.A., Tounsi, A. and Mahmoud, S. (2019), "Static and dynamic behavior of (FG-CNT) reinforced porous sandwich plate using energy principle", *Steel Compos. Struct.*, **32**(5), 595-610. https://doi.org/10.12989/scs.2019.32.5.595.

Mirjavadi, S.S., Matin, A., Shafiei, N., Rabby, S. and Mohasel Afshari, B. (2017a), "Thermal buckling behavior of two-dimensional imperfect functionally graded microscale-tapered porous beam", *J. Therm. Stresses.*, **40**(10), 1201-1214. http://doi.org/10.1080/01495739.2017.1332962.

Mirjavadi, S.S., Rabby, S., Shafiei, N., Afshari, B.M. and Kazemi, M. (2017b), "On size-dependent free vibration and thermal buckling of axially functionally graded nanobeams in thermal environment", *Appl. Phys. A.*, **123**(5), 315. http://doi.org/10.1007/s00339-017-0918-1.

Moayedi, H., Habibi, M., Safarpour, H., Safarpour, M. and Foong, L.K. (2019), "Buckling and frequency responses of a graphene nanoplatelet reinforced composite microdisk", *Int. J. Appl. Mech.*, **11**(10), 1950102. http://doi.org/10.1142/s1758825119501023.

Moradi, Z., Davoudi, M., Ebrahimi, F. and Ehyaei, A.F. (2021), "Intelligent wave dispersion control of an inhomogeneous micro-shell using a proportional-derivative smart controller", *Wave. Random Complex.*, 1-24. http://doi.org/10.1080/17455030.2021.1926572.

Navi, B.R., Mohammadimehr, M. and Arani, A.G. (2019), "Active control of three-phase CNT/resin/fiber piezoelectric polymeric nanocomposite porous sandwich microbeam based on sinusoidal shear deformation theory", *Steel Compos. Struct.*, **32**(6), 753-767. https://doi.org/10.12989/scs.2019.32.6.753.

Nejadi, M.M. and Mohammadimehr, M. (2020), "Buckling analysis of nano composite sandwich Euler-Bernoulli beam considering porosity distribution on elastic foundation using DQM", *Adv. Nano Res.*, **8**(1), 59-68. https://doi.org/10.12989/anr.2020.8.1.059.

Reddy, J.N. (2011), "Microstructure-dependent couple stress theories of functionally graded beams", *J. Mech. Phys. Solids.*, **59**(11), 2382-2399. https://doi.org/10.1016/j.jmps.2011.06.008.

Safarpour, M., Ghabussi, A., Ebrahimi, F., Habibi, M. and Safarpour, H. (2020), "Frequency characteristics of FG-GPLRC viscoelastic thick annular plate with the aid of GDQM", *Thin Wall. Struct.*, **150**, 106683. https://doi.org/10.1016/j.tws.2020.106683.

Semmah, A., Heireche, H., Bousahla, A.A. and Tounsi, A. (2019), "Thermal buckling analysis of SWBNNT on Winkler foundation by non local FSDT", *Adv. Nano Res.*, **7**(2), 89-98. http://doi.org/10.12989/anr.2019.7.2.089.

Shafiei, N., Kazemi, M. and Ghadiri, M. (2016a), "Nonlinear vibration behavior of a rotating nanobeam under thermal stress using Eringen's nonlocal elasticity and DQM", *Appl. Phys. A*, **122**(8), 728. http://doi.org/10.1007/s00339-016-0245-y.

Shafiei, N., Kazemi, M. and Ghadiri, M. (2016b), "Nonlinear vibration of axially functionally graded tapered microbeams", *Int. J. Eng. Sci.*, **102**, 12-26. https://doi.org/10.1016/j.ijengsci.2016.02.007.

Shafiei, N., Kazemi, M., Safi, M. and Ghadiri, M. (2016c), "Nonlinear vibration of axially functionally graded non-uniform nanobeams", *Int. J. Eng. Sci.*, **106**, 77-94. https://doi.org/10.1016/j.ijengsci.2016.05.009.

Shafiei, N., Kazemi, M. and Ghadiri, M. (2016d), "Nonlinear vibration behavior of a rotating nanobeam under thermal stress using Eringen's nonlocal elasticity and DQM", *Appl. Phys. A*, **122**(8), 728. http://doi.org/10.1007/s00339-016-0245-y.

Shafiei, N., Kazemi, M. and Ghadiri, M. (2016e), "Nonlinear vibration of axially functionally graded tapered microbeams", *Int. J. Eng. Sci.*, **102**, 12-26. https://doi.org/10.1016/j.ijengsci.2016.02.007.

Shafiei, N., Kazemi, M., Safi, M. and Ghadiri, M. (2016f), "Nonlinear vibration of axially functionally graded non-uniform nanobeams", *Int. J. Eng. Sci.*, **106**, 77-94. https://doi.org/10.1016/j.ijengsci.2016.05.009.

Shafiei, N., Mousavi, A. and Ghadiri, M. (2016g), "On size-dependent nonlinear vibration of porous and imperfect functionally graded tapered microbeams", *Int. J. Eng. Sci.*, **106**, 42-56. https://doi.org/10.1016/j.ijengsci.2016.05.007.

Shafiei, N. and Kazemi, M. (2017), "Nonlinear buckling of functionally graded nano-/micro-scaled porous beams", *Compos. Struct.*, **178**, 483-492. https://doi.org/10.1016/j.compstruct.2017.07.045.

Shafiei, N., Mirjavadi, S.S., Afshari, B.M., Rabby, S. and Hamouda, A.M.S. (2017a), "Nonlinear thermal buckling of axially functionally graded micro and nanobeams", *Compos. Struct.*, **168**, 428-439. https://doi.org/10.1016/j.compstruct.2017.02.048.

Shafiei, N., Ghadiri, M., Makvandi, H. and Hosseini, S.A. (2017b), "Vibration analysis of Nano-Rotor's Blade applying Eringen nonlocal elasticity and generalized differential quadrature method", *Appl. Math. Model.*, **43**, 191-206. https://doi.org/10.1016/j.apm.2016.10.061.

Shafiei, N., Ghadiri, M. and Mahinzare, M. (2019), "Flapwise bending vibration analysis of rotary tapered functionally graded nanobeam in thermal environment", *Mech. Adv. Mater. Struct.*, **26**(2), 139-155. http://doi.org/10.1080/15376494.2017.1365982.

Shafiei, N., Hamisi, M. and Ghadiri, M. (2020), "Vibration analysis of rotary tapered axially functionally graded Timoshenko nanobeam in thermal environment", *J. Solid Mech.*, **12**(1), 16-32. http://doi.org/10.22034/jsm.2019.563759.1273.

Shariati, A., Ghabussi, A., Habibi, M., Safarpour, H., Safarpour, M., Tounsi, A. and Safa, M. (2020a), "Extremely large oscillation and nonlinear frequency of a multi-scale hybrid disk resting on nonlinear elastic foundation", *Thin Wall. Struct.*, **154**, 106840. https://doi.org/10.1016/j.tws.2020.106840.

Shariati, A., Jung, D.W., Mohammad-Sedighi, H., Żur, K.K., Habibi, M. and Safa, M. (2020b), "Stability and dynamics of viscoelastic moving rayleigh beams with an asymmetrical distribution of material parameters", *Symmetry*, **12**(4), 586. https://doi.org/10.3390/sym12040586.

Sheng, H., Wang, S., Zhang, Y., Yu, D., Cheng, X., Lyu, W. and Xiong, Z. (2021), "Near-online tracking with co-occurrence constraints in blockchain-based edge computing", *IEEE Internet Thing J.*, **8**(4), 2193-2207. http://doi.org/10.1109/JIOT.2020.3035415.

Shokrgozar, A., Ghabussi, A., Ebrahimi, F., Habibi, M. and Safarpour, H. (2020), "Viscoelastic dynamics and static responses of a graphene nanoplatelets-reinforced composite cylindrical microshell", *Mech. Based Des. Struct.*, 1-28. http://doi.org/10.1080/15397734.2020.1719509.

Tahir, S.I., Chikh, A., Tounsi, A., Al-Osta, M.A., Al-Dulaijan, S.U. and Al-Zahrani, M.M. (2021a), "Wave propagation analysis of a ceramic-metal functionally graded sandwich plate with different porosity distributions in a hygro-thermal environment", *Compos. Struct.*, **269**, 114030. https://doi.org/10.1016/j.compstruct.2021.114030.

Tahir, S.I., Tounsi, A., Chikh, A., Al-Osta, M.A., Al-Dulaijan, S.U. and Al-Zahrani, M.M. (2021b), "An integral four-variable hyperbolic HSDT for the wave propagation investigation of a ceramic-metal FGM plate with various porosity distributions resting on a viscoelastic foundation", *Wave. Random Complex*, 1-24. http://doi.org/10.1080/17455030.2021.1942310.

Wang, H., Zandi, Y., Gholizadeh, M. and Issakhov, A. (2021), "Buckling of porosity-dependent bi-directional FG nanotube using numerical method", *Adv. Nano Res*., **10**(5), 493-507. https://doi.org/10.12989/anr.2021.10.5.493.

Wu, Z., Song, A., Cao, J., Luo, J. and Zhang, L. (2020), "Efficiently translating complex SQL query to MapReduce jobflow on cloud", *IEEE T. Cloud Comput*., **8**(2), 508-517. http://doi.org/10.1109/TCC.2017.2700842.

Xie, J., Chen, Y., Yin, L., Zhang, T., Wang, S. and Wang, L. (2021), "Microstructure and mechanical properties of ultrasonic spot welding TiNi/Ti6Al4V dissimilar materials using pure Al coating", *J. Manuf. Proc*., **64**, 473-480. https://doi.org/10.1016/j.jmapro.2021.02.009.

Yang, F., Chong, A.C.M., Lam, D.C.C. and Tong, P. (2002), "Couple stress based strain gradient theory for elasticity", *Int. J. Solids Struct*., **39**(10), 2731-2743. https://doi.org/10.1016/S0020-7683(02)00152-X.

Yang, J. and Shen, H.S. (2002), "Vibration characteristics and transient response of shear-deformable functionally graded plates in thermal environments", *J. Sound Vib*., **255**(3), 579-602. https://doi.org/10.1006/jsvi.2001.4161.

Zhang, C., Jin, Q., Song, Y., Wang, J., Sun, L., Liu, H., Dun, L., Tai, H., Yuan, X., Xiao, H., Zhu, L. and Guo, S. (2021a), "Vibration analysis of a sandwich cylindrical shell in hygrothermal environment", *Nanotechnol. Rev*., **10**(1), 414-430. https://doi.org/10.1515/ntrev-2021-0026.

Zhang, T., Wu, X., Shaheen, S.M., Rinklebe, J., Bolan, N.S., Ali, E.F., Li, G. and Tsang, D.C.W. (2021b), "Effects of microorganism-mediated inoculants on humification processes and phosphorus dynamics during the aerobic composting of swine manure", *J. Hazard. Mater*., **416**, 125738. https://doi.org/10.1016/j.jhazmat.2021.125738.

Zhao, N., Deng, L., Luo, D. and Zhang, P. (2020), "One-step fabrication of biomass-derived hierarchically porous carbon/MnO nanosheets composites for symmetric hybrid supercapacitor", *Appl. Surf. Sci*., **526**, 146696. https://doi.org/10.1016/j.apsusc.2020.146696.

Zhao, Y., Moradi, Z., Davoudi, M. and Zhuang, J. (2021), "Bending and stress responses of the hybrid axisymmetric system via state-space method and 3D-elasticity theory", *Eng. Comput*., 1-23. http://doi.org/10.1007/s00366-020-01242-1.

Zine, A., Bousahla Abdelmoumen, A., Bourada, F., Benrahou Kouider, H., Tounsi, A., Adda Bedia, E.A., Mahmoud, S.R. and Tounsi, A. (2020), "Bending analysis of functionally graded porous plates via a refined shear deformation theory", *Comput. Concrete*, **26**(1), 63-74. http://doi.org/10.12989/CAC.2020.26.1.063.